

# Modeling and Simulation of Heat Transfer Phenomenon in Steel Belt Conveyer Sulfur Granulating Process

*Abdoli Rad, Mayam; Shahsavand, Akbar\*<sup>+</sup>*

*Chemical Engineering Department, Faculty of Engineering, Ferdowsi University of Mashhad,  
P.O. Box 91775-1111 Mashhad, I.R. IRAN*

**ABSTRACT:** *Complex heat transfer phenomena (including unsteady state conduction, convection and solidification processes) occur in steel belt conveyer sulfur granulating method. Numerical simulation of this technique is performed via a comprehensive and multifaceted one dimensional model. Since the air situated between the adjacent sulfur pastilles is essentially stagnant, therefore, the surface temperatures of neighboring pastilles are actually the same during cooling process and the radial heat transfer can be entirely ignored. Knowing this issue, the axial heat flow is the only remaining mechanism of heat transfer and the one dimensional model would be valid. After solving the partial differential equation of the model, the effects of various operating conditions (such as ambient air temperature, inlet cooling water flow rate and its temperature, initial temperature of the liquid sulfur droplet and steel belt conveyer speed) are studied on the performance of the entire granulation process. According to results, with increasing the cooling water flow rate and steel belt conveyer speed, solidification rate of the liquid sulfur droplet is increased. Furthermore, the solidification process of the sulfur droplet occurs more rapidly when the ambient air temperature, initial liquid sulfur temperature and inlet water temperature are reduced. To the best of our knowledge, simulation of steel belt conveyer sulfur granulating process has not been addressed previously.*

**KEY WORDS:** *Sulfur, Granulating, Modeling, Rotary steel belt, One dimensional.*

## INTRODUCTION

Granulation of dusty materials makes it possible to solve many environmental problems. Elemental sulfur should be granulated because this process improves its physicochemical properties for easier handling. Hence, according to wide demand of sulfur in different industries the tendency for granulation of sulfur increased in the past few decades [1].

Various methods are available for granulating of sulfur in which liquid sulfur is solidified in different

ways. In the Air cooling process, liquid sulfur is sprayed into an upward flow of air. This process provides high quality sulfur granules but it is relatively expensive and a large amount of sulfur is carried away from tower by air which pollutes the environment [1].

Sulfur granules can also be obtained by wet granulating process. This process is more economical, but it suffers from discarding large quantities of wastewater due to direct contact between sulfur and cooling water [2].

\* To whom correspondence should be addressed.

+ E-mail: shahsavand@um.ac.ir

1021-9986/13/4/93

12/\$/3.20

Another sulfur granulation process is spray granulating process. This method is not appropriate because of its explosion hazards [1]. In another technique, liquid sulfur can be cooled by rotary steel belt cooling granulating process. In this process, a distributor splits up liquid sulfur into several droplets where they are placed on the steel belt conveyer. Cooling water is sprayed on the other side of steel belt and ambient air also cools down the granulated sulfur from above. The liquid drops are solidified and formed due to simultaneous heat transfer between sulfur pastilles and the surrounding fluids [1,3].

Each granulating process has its own advantages and drawbacks. The selected method should satisfy different production requirements. Appropriate moisture content, friability and Particle Size Distribution (PSD) of granules are amongst the main important parameters required for optimal operation [1]. The most important advantages of rotary steel belt cooling granulating process are: 1) uniform particle sizes 2) low moisture content 3) being environment-friendly 4) economical operation. So among of other sulfur granulating processes, Rotary steel belt cooling granulating process is usually considered as the best method [3].

Numerical simulation of various engineering process has been received severe attention the present millenium [4-10] while tremendous modeling has been performed on the solidification of molten metal droplets by spray forming [11,12], on a cooled substrate [13] and impacting onto solid substrate [14]. However, there is a severe shortage of academic articles on detailed description or modeling of various sulfur granulating processes. Amongst a few, the following researches provide useful information about the fabrication techniques or modeling of the granulation processes.

The first technology of forming liquid sulfur was the sulfur slating process developed by *Vennard & Ellithorpe* in the early 1970s, however this process is obsolete and slates are no longer used for granulation purposes [15].

The original inventor of wet granulating process was Ron Fletcher and it was developed in 1978 by Enersul group [15]. There are several inventions related to wet granulating process which are fully described in several patents [16,17].

Air cooling granulating process was initially commercialized in Finland about 40 years ago. It ceased

to operate in 1977 [1]. This process was also known as Polish Air Prilling Process. In early eighties, air cooling granulating captured around 57% of the international world sulfur market [2]. This method was the subject of several patents [18-21].

Spray granulating process (GX<sup>TM</sup> granulating) was developed in Alberta at the Harmattan and Windfall gas plants in 1979. A new version was designed at Crossfield in 1983, and all of these facilities operated until early 1990s. These granulation processes weren't in operation in Alberta until 2004-2005 when Enersul group began to upgrade its sulfur forming facilities in Western Canada [22]. Rotary steel belt granulating process was developed between the late 1980s and the early 1990s by *Sandvik*. In 2005, *Sandvik* developed high speed rotary steel belt for high capacity [23].

Due to complex nature of granulation process, only one modeling article has been presented for wet granulating method. The effect of temperature regimes on various qualitative characteristics of granules (produced by the wet process) was studied via numerical simulation. The simulation results showed proper agreement with experimental data [24,25]. No other modeling of any granulation process was found in the literature.

A comprehensive review of various sulfur granulating techniques is presented in the present article. Rotary steel belt cooling granulating process is selected as the optimal unit due to its numerous optimal characteristics and its versatile applications. A mathematical procedure is presented for modeling of rotary steel belt cooling granulation process. Finite difference technique (usually known as Forward Time Central Space (FTCS) [26]) is used to solve the one dimensional mathematical model of the pastille solidification process. The effect of various operating parameters will be investigated on the overall performance of the granulation process.

## THEORITICSL SECTION

### *Description of optimized sulfur Granulation process*

As shown in Fig. 1, liquid sulfur at around 145°C was received from Sulfur Recovery Unit (SRU). It is then converted to uniform droplets via rotoform and distributed evenly on the rotary steel belt conveyer. Afterward, liquid sulfur droplets are cooled, solidified and formed by cooling water which is sprayed

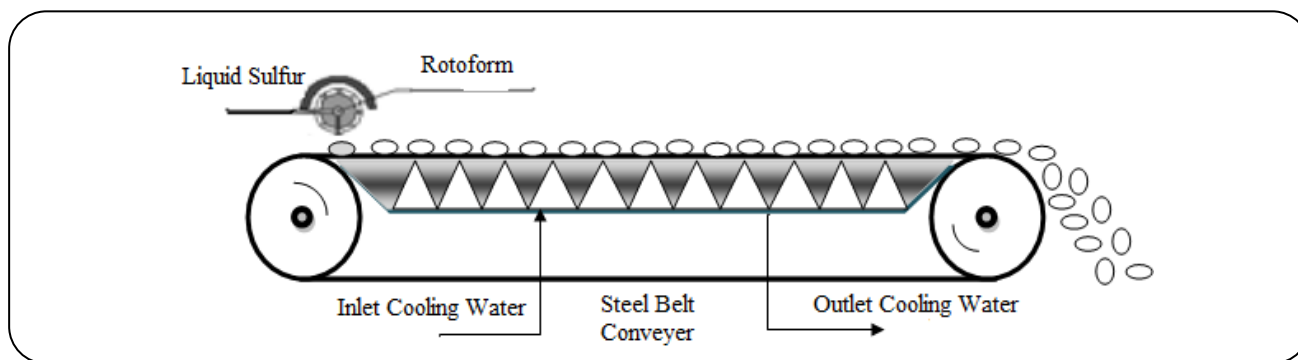


Fig. 1: Schematic diagram of rotary steel belt cooling granulation process.

on the underside of steel belt via heat conduction and also ambient air which is above the steel belt conveyer via heat convection as they are being conveyed. At no stage will the cooling water come in contact with the sulfur. The rotary steel belt conveyer changes its direction at discharge end to facilitate peeling process.

The overall cooling process can be divided into four distinct stages. Initially, liquid sulfur droplet is cooled down by both cooling water (from belt side) and ambient air (from top) until one of its faces reaches the solidification point temperature ( $T_m$ ). Afterwards, Cooling of the sulfur droplet continues until another face reaches the same solidification point temperature ( $T_m$ ). In the third stage, solidification zones from both sides grow incrementally until they meet each other at a certain middle point where the solidification temperature ( $T_m$ ) prevails. Evidently, the sulfur droplet becomes entirely solid at this point. Therefore, at the final stage the solid sulfur pastille cools down until it leaves the steel belt conveyer. Fig. 2 shows the typical schematic temperature profiles inside the pastille at the above four stages. Various times are denoted in Figure 2 will be described in more details in the next section.

#### Modeling of sulfur granulation process

The object of this investigation is to estimate the variation of temperature profile inside an individual sulfur droplet with cooling time. The distribution of temperature across the pastille determines the qualitative characteristics of the produced granule. The following assumptions are made to simplify the rather complex model of the cooling process:

- The pastille is similar to a coin with a diameter of  $d_p$  and height of  $l_p$ .

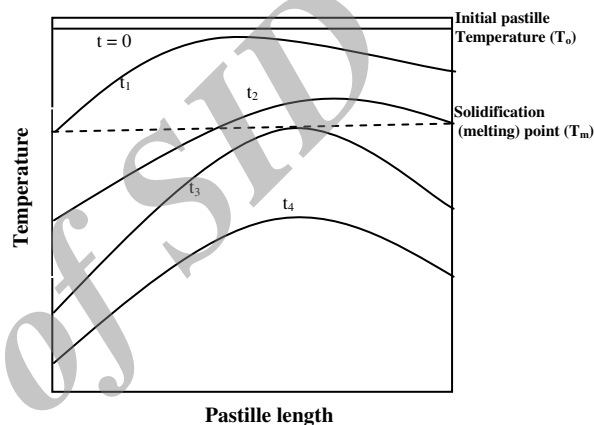


Fig. 2: Schematic representation of four different cooling stages.

- Heat transfer in radial axis is neglected (one dimensional temperature profile).
- Constant physical properties
- Constant belt speed
- Constant heat flux from underside of the belt conveyer ( $q'' = (\dot{m} C_p (T_{wout} - T_{win})) / A$ )
- Constant ambient air temperature ( $T_{air}$ )

In this case, the dynamics of the thermal processes in the sulfur droplet is described by a system of differential, unsteady heat-conduction equations. For the case of constant physical properties of the solid and liquid phases, the system of differential equations in the axial dimension cylindrical coordinate system can be simplified as [27]:

$$\frac{\partial T}{\partial t} = \alpha \left[ \frac{\partial^2 T}{\partial z^2} \right] + Q / C_p \quad (1)$$

where,  $Q$  denotes the released heat flux rate (J/kg.s)

due to solidification process. Evidently, in the absence of solidification, the second right hand side term vanishes. Assuming that solidification starts at belt face (which is the more frequent case), then the initial values and the corresponding boundary conditions can be summarized as following:

Stage 1) Cooling of liquid sulfur droplet ( $0 \leq t < t_1$ ):

$$\begin{aligned} [t = 0] \quad & T_{(z,0)} = T_0 \\ [z = 0] \quad & k_1 \frac{dT_{(0,t)}}{dz} = q'' = \frac{C_p (T_{wout} - T_{win})}{A} \\ [z = l_p] \quad & h(T_{(lp,t)} - T_{air}) = k_1 \frac{dT_{(lp,t)}}{dz} \end{aligned}$$

Stage 2) Cooling of sulfur pastille after solidification starts at belt face ( $t_1 \leq t < t_2$ ):

$$\begin{aligned} [t = t_1 \text{ and } z = 0] \quad & k_{sl} \frac{dT_{(0,t)}}{dz} + Q/A = q'' \\ \text{Otherwise } (z = 0) \quad & k_1 \frac{dT_{(0,t)}}{dz} = q'' = \frac{C_p (T_{wout} - T_{win})}{A} \\ [z = l_p] \quad & \text{same as stage 1} \end{aligned}$$

Stage 3) Cooling of sulfur pastille after solidification starts at other face ( $t_2 \leq t < t_3$ ):

$$\begin{aligned} [Z = 0] \quad & k_s \frac{dT_{(0,t)}}{dz} = q'' = \frac{C_p (T_{wout} - T_{win})}{A} \\ [t = t_2 \text{ and } z = l_p] \quad & h(T_{(lp,t)} - T_{air}) = k_{sl} \frac{dT_{(lp,t)}}{dz} + Q/A \\ \text{Otherwise } (z = l_p) \quad & h(T_{(lp,t)} - T_{air}) = k_s \frac{dT_{(lp,t)}}{dz} \end{aligned}$$

Stage 4) Cooling of solid sulfur granule ( $t_3 \leq t \leq t_{max}$ ):

$$\begin{aligned} [Z = 0] \quad & k_s \frac{dT_{(0,t)}}{dz} = q'' = \frac{C_p (T_{wout} - T_{win})}{A} \\ [z = l_p] \quad & h(T_{(lp,t)} - T_{air}) = k_s \frac{dT_{(lp,t)}}{dz} \end{aligned}$$

The heat transfer coefficient is calculated from the following empirical equation [28]:

$$Nu = 0.664 Re^{0.5} Pr^{\frac{1}{3}} \quad (2)$$

The system of differential equations is then solved numerically by the FTCS method to provide the dynamic behavior of a given sulfur pastille. The required temperature profiles across the pastille at different instants are computed using a computer program in the MATLAB environment. Fig. 3 illustrates the detailed computational steps required for the recruited simulation procedure.

### A practical case study

The proposed model is applied to sulfur granulating process of Khangiran refinery. The unit receives around 300 tons per day liquid sulfur and converts it to sulfur pastilles using a rotary steel belt granulating process. Table 1 illustrates the base operating conditions and other required information for the simulation of sulfur granulation process (mostly borrowed from the Khangiran refinery sulfur granulating process). The one dimensional model of Fig. 3 was used along with the data of Table 1 to simulate the sulfur granulating process for a single liquid sulfur droplet.

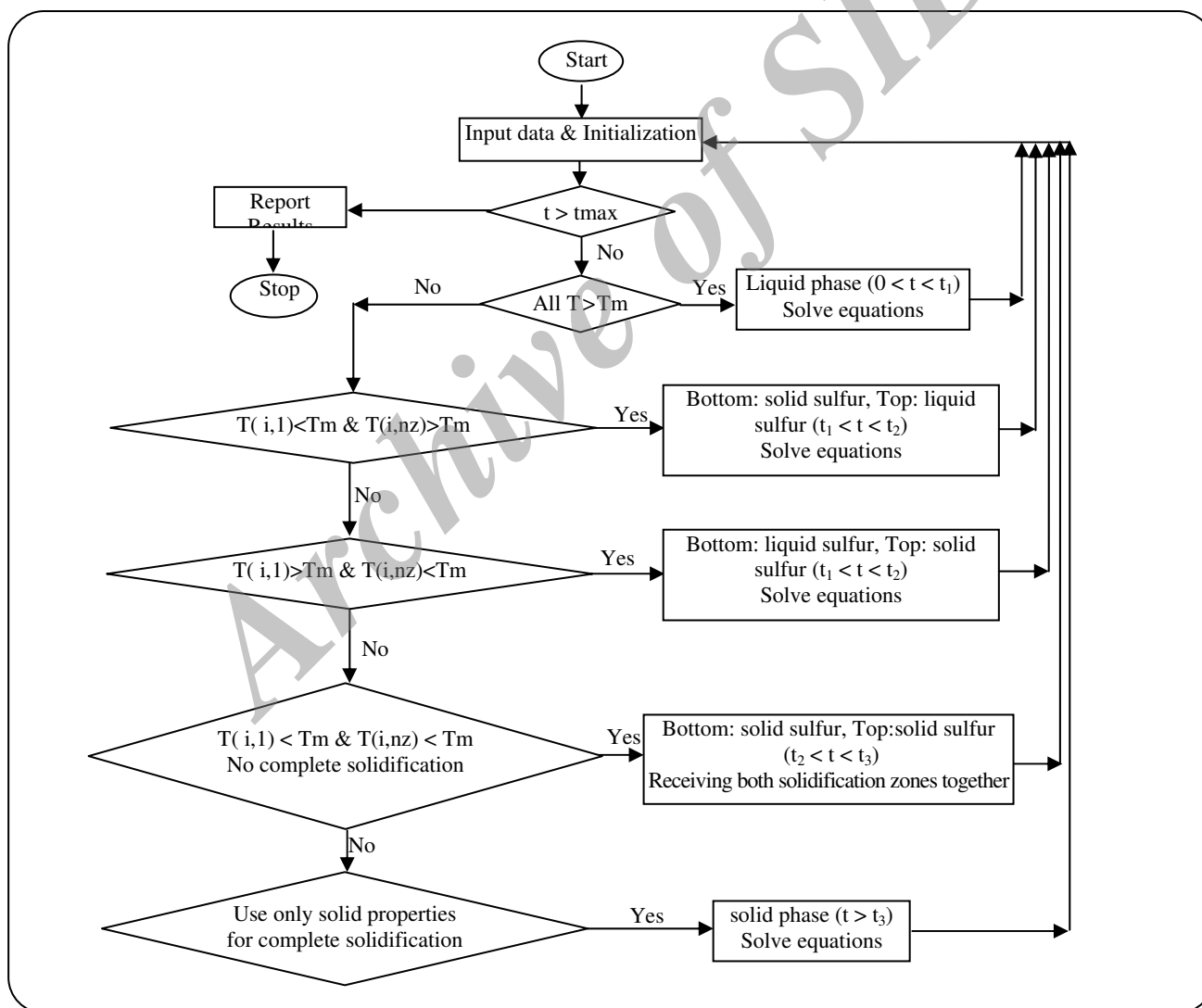
## RESULTS AND DISCUSSIONS

Fig. 4 presents various computed axial temperature profiles of the sulfur droplet for the base case (of Table 1) in four separate stages (as described previously) and 2 additional conditions (at  $t=0$ ,  $T_0=418K$  and  $t=5s$ ) for comparison intentions. Initially, liquid sulfur droplet is cooled by both cooling water (sprayed under belt side) and ambient air (from the top side) until one of its faces reaches the solidification point temperature ( $T_m$ : represented by dotted line at  $390K$ ). The time between the placement of liquid sulfur droplet on the steel belt and solidification of one of its faces (belt side face, for this case) is denoted by  $t_1 = 0.27s$ .

Afterwards, cooling of the sulfur droplet continues until another face (air side face, for this case) reaches the solidification point temperature and the time at this moment is denoted by  $t_2=0.71 s$ . Thereafter, solidification zones from both sides grow until they meet each other and droplet temperature reaches solidification point. At some point in the middle of the droplet. At this point the sulfur droplet becomes entirely solid and the corresponding time is recorded as  $t_3= 2.48s$ . Finally, the solid sulfur granule cools down until it leaves

**Table 1: Base operating conditions and supplementary information required for simulation.**

Parameter	Value
Initial liquid sulfur temperature	145 °C
Ambient air temperature ( $T_{air}$ )	30 °C
Steel belt conveyer speed ( $V_{belt}$ )	0.5 m/s
Steel belt conveyer length (L)	5 m
Steel belt conveyer width (W)	0.5 m
Mid time ( $t_{mid}$ )	5 s
Maximum time ( $t_{max}=L/V_{belt}$ )	10 s
Temperature of inlet cooling water ( $T_{win}$ )	25 °C
Calculated cooling water outlet temperature ( $T_{wout}$ )	27 °C
Cooling water flow rate ( $Q_w$ )	8 L/s
Diameter of pastille ( $d_p$ )	4 mm
Height of pastille ( $l_p$ )	1.6 mm

**Fig. 3: One dimensional modeling flowchart of sulfur granulation.**

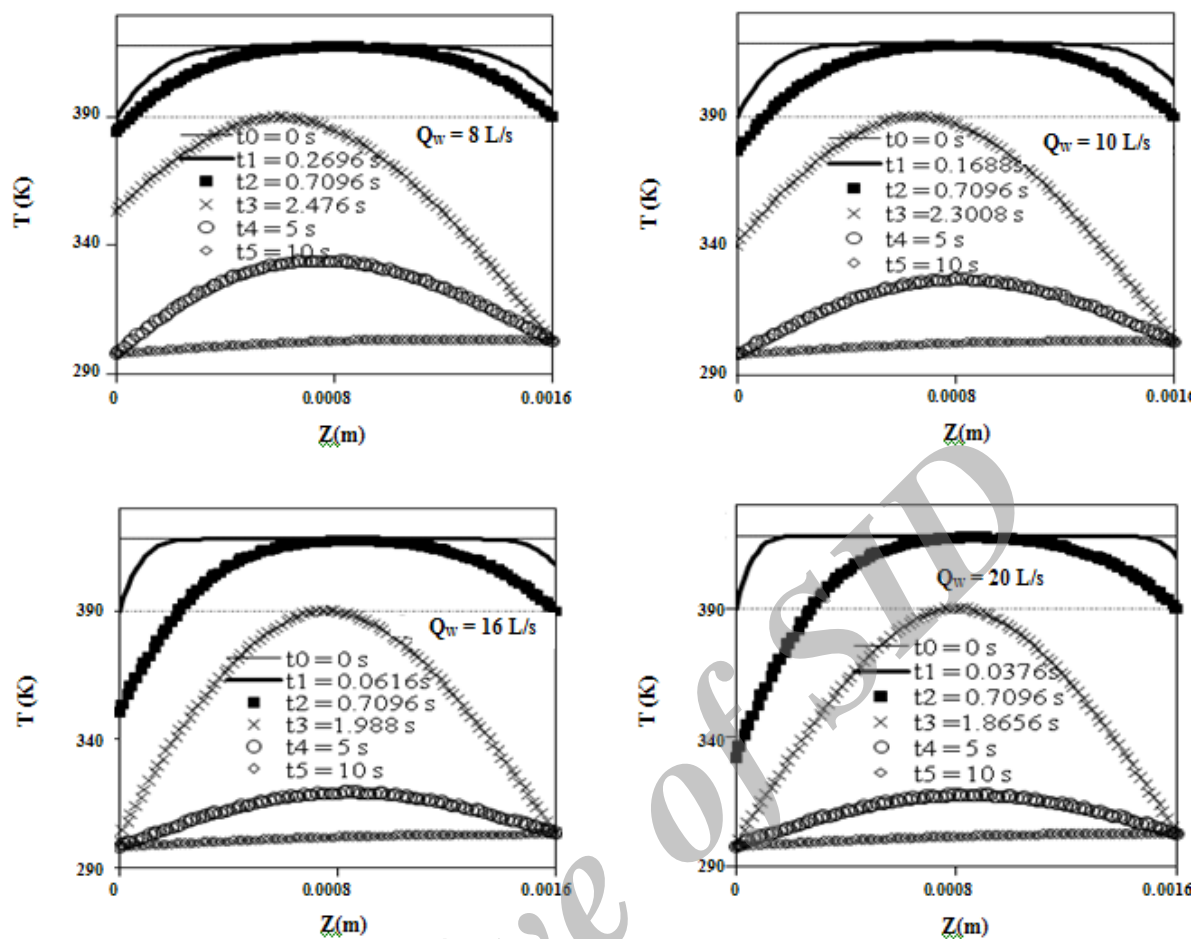


Fig. 5: Various sulfur pastille temperature profiles for different cooling water flow rates.

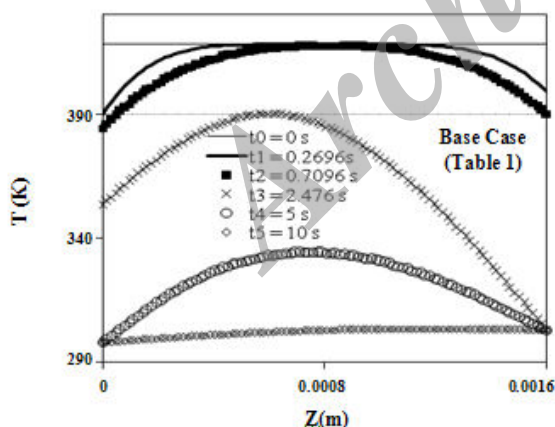


Fig. 4: temperature of sulfur droplet vs. length of pastille.

the steel belt conveyor at  $t_{\max} = 10$  seconds after the start of granulation process. Temperature profile of the sulfur droplet at  $t_{\text{mid}} = t_4 = 5 \text{ s}$  is also shown for comparison

purposes. As it can be seen, the axial temperature profile reaches its final value after about 10 seconds.

To study the effect of various operating parameters (such as cooling water flow rate, ambient air temperature, initial liquid sulfur temperature, inlet water temperature and steel belt conveyor speed) on the performance of the overall granulation process, the simulation was repeated several times when only one parameter was changed at a time and all other operating conditions were kept constant.

Fig. 5 shows the simulation results when the cooling water flow rate was increased from its initial value of  $Q_w = 8 \text{ L/s}$  at base point to  $Q_w = 20 \text{ L/s}$  in four steps. As expected, increasing the cooling water flow rate causes Severe decrease in  $t_1$  but it doesn't affect  $t_2$ , because the air temperature and the speed of the belt conveyor control the latter time  $t_2$ . On the other hand,

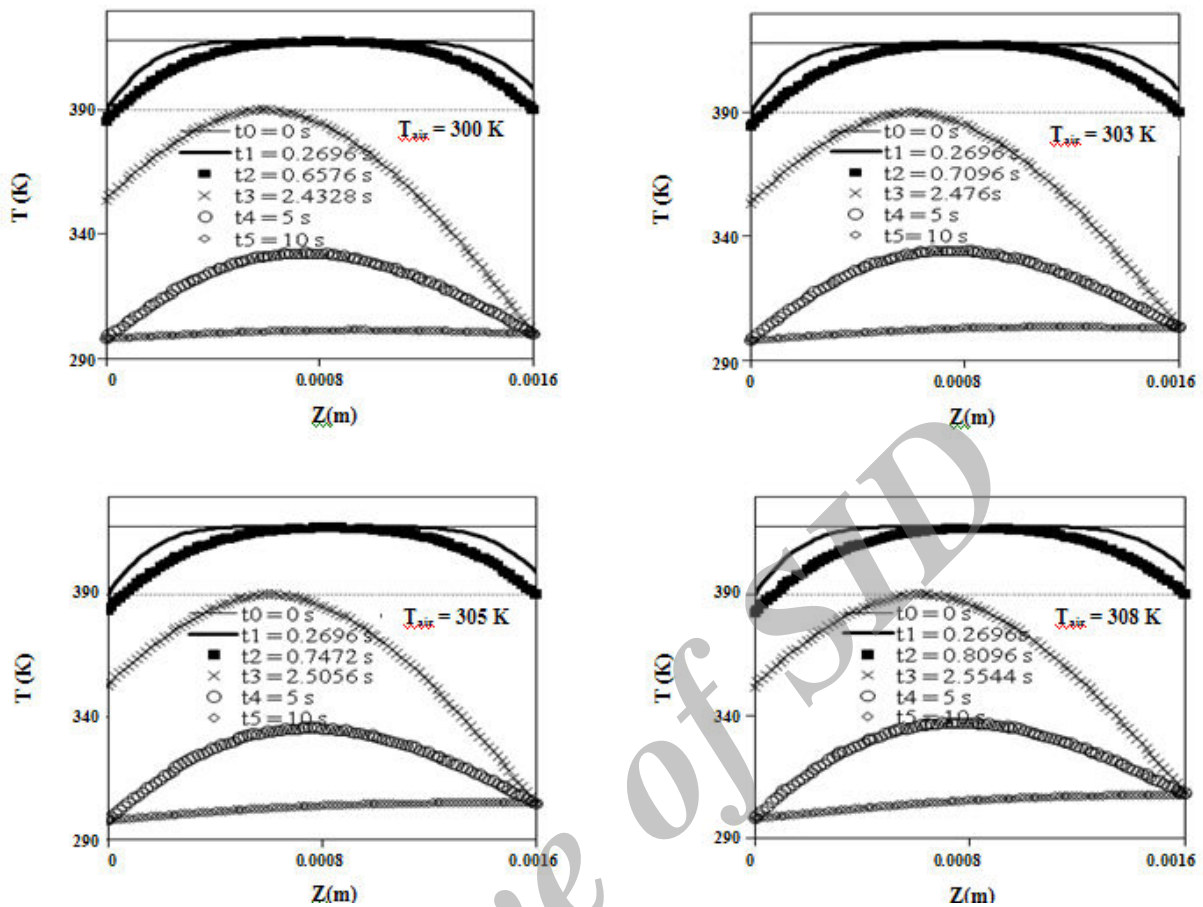


Fig. 7: Various sulfur pastille temperature profiles for different ambient air temperatures.

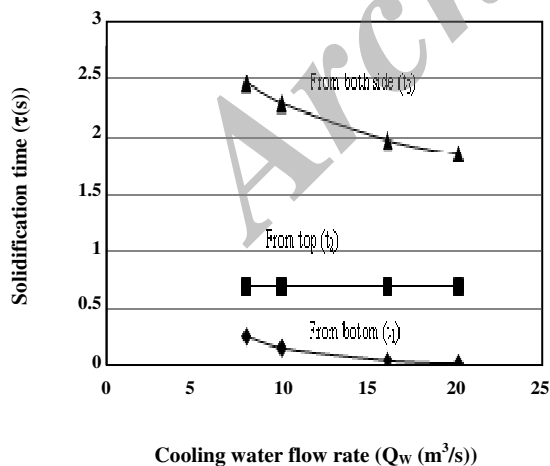


Fig. 6: Effect of cooling water flow rate increase on the temperature profiles of sulfur pastille.

an increase in cooling water rate will decrease  $t_3$  because more rapid heat dissipation from the belt face will lead to faster solidification of the bottom layer which pulls away the latest solidification point from belt side and pushes it towards the air face. Once again, the axial temperature profile reaches its final value for all cases, after about 10 seconds and temperature profile at  $t_{mid}=t_4 = 5s$  is shown for comparison purposes.

As explained earlier, increasing cooling water flow rate decreases  $t_1$  and  $t_3$  but it does not affect  $t_2$ . This point is clearly illustrated in Fig. 6. Note that, increasing in cooling water flow rate has more pronounced effect on  $t_3$  than  $t_1$ , because  $t_3$  is usually much larger than  $t_1$ .

Fig. 7 shows the simulation results when the ambient air temperature is increased from its initial value of  $T_{air} = 300K$  to  $T_{air}=308K$  in four distinct steps. All other parameters (cooling water flow rate, initial liquid sulfur

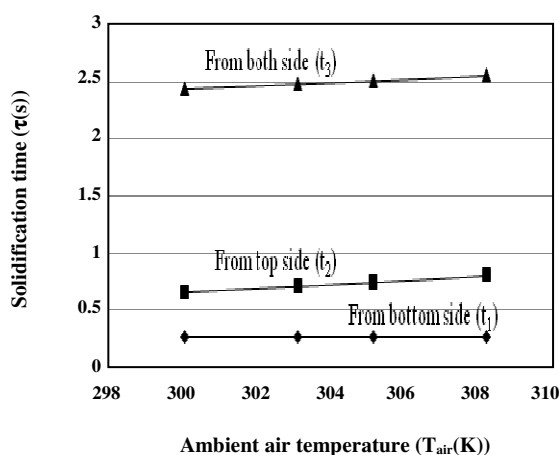


Fig. 8: Effect of ambient air temperature increase on the temperature profiles of sulfur pastille.

temperature, inlet water temperature and steel belt speed) are kept constant. As it can be seen, increasing air temperature causes a severe increase in  $t_2$  but it doesn't affect  $t_1$ . Furthermore, as shown in Fig. 8, an increase in ambient air temperature will increase  $t_3$  because less rapid heat dissipation from the air face will lead to slower solidification of the top layer which pulls away the very last solidification point from belt side and pushes it towards air side. As before, all axial temperature profiles reach their final value after about 10 seconds and temperature profile at  $t_{mid}=t_4 = 5s$  is also shown for comparison purposes.

Fig. 9 shows the computed axial temperature profile of the sulfur droplet when the initial temperature of sulfur droplet is increased from  $T_0= 403K$  to  $T_0= 418K$  in several steps while all other parameters (cooling water flow rate, ambient air temperature, inlet water temperature and steel belt speed) are kept constant. Obviously, more time is required to solidify sulfur droplet when initial liquid sulfur temperature is increased. In other words, the required solidification times for all stages ( $t_1$ ,  $t_2$  and  $t_3$ ) will increase with increasing the initial temperature of sulfur droplet as clearly shown in Fig. 10.

In a similar manner, Fig. 11 illustrates the simulation results when the inlet cooling water temperature is increased from its initial value of  $T_{win}= 288 K$  to  $T_{win}= 298 K$  in four distinct intervals. All other parameters (cooling water flow rate, initial liquid sulfur

temperature, ambient air temperature and steel belt speed) are kept constant.

Evidently, increasing inlet water temperature causes a severe increase in  $t_1$  but it doesn't affect  $t_2$ . Furthermore, as shown in Fig. 12, an increase in inlet water temperature will increase  $t_3$  because less rapid heat dissipation from the belt face will lead to slower solidification of the bottom layer which pulls away the very last solidification point from air side and pushes it towards belt side.

As it is illustrated in Fig. 13, steel belt speed is increased from its initial value of  $V_{belt}= 0.1 m/s$  to  $V_{belt}= 1 m/s$  in four steps. Other operating parameters (cooling water flow rate, ambient air temperature, inlet water temperature and initial liquid sulfur temperature) are again kept constant. Obviously, with increasing steel belt speed, the initial time interval ( $t_1$ ) remains constant but the second time interval ( $t_2$ ) decreases very rapidly. The reason for these different behaviors lies in the fact that the first time increment ( $t_1$ ) is controlled by the inlet water temperature and flow rate and does not depend on conveyer speed. On the other hand, increasing steel belt conveyer speed amplifies the convective heat transfer coefficient between pastille and ambient air which leads to faster heat dissipation from the air face so rapid solidification occurs which requires much less times ( $t_2$  and  $t_3$ ). In other words, increasing the belt conveyer speed pushes last solidification point from air side towards the belt side. This point is clearly demonstrated in Fig. 14.

## CONCLUSIONS

An extensive one dimensional heat transfer model was presented and employed to simulate the solidification of a single liquid sulfur droplet for steel belt sulfur granulating process using MATLAB software environment. The operating conditions and other supplementary data were borrowed from the sulfur granulation process of Khangiran sour gas refinery (Northeast of Iran). It was clearly shown that the performance of the entire granulating process strongly depends on various operating conditions, such as ambient air temperature, cooling water flow rate and initial liquid sulfur temperature. Increasing the cooling water flow rate and steel belt conveyer speed led to an increase in the solidification rate of the liquid sulfur droplet from



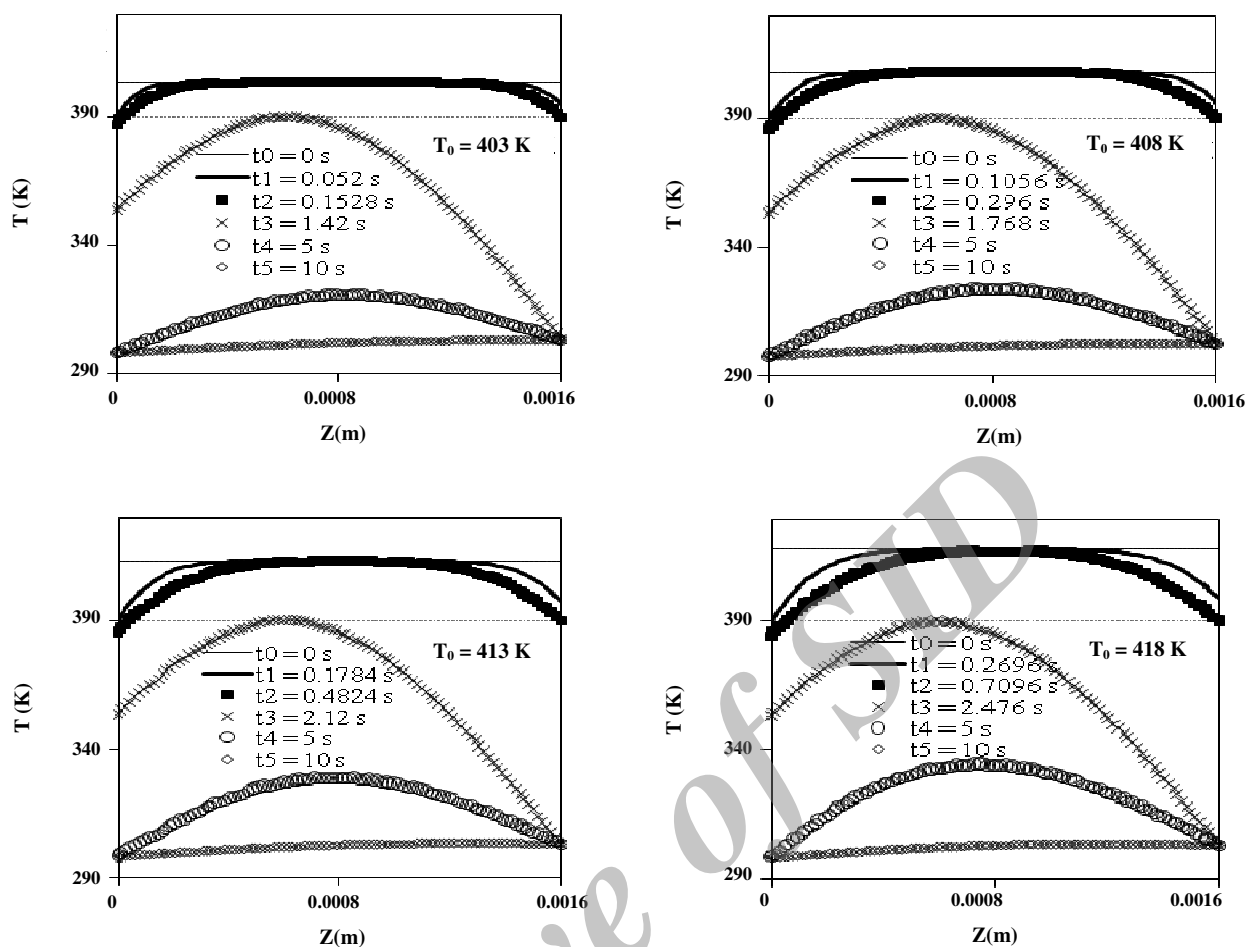


Fig. 9: Various sulfur pastille temp. profiles for different initial temperatures of sulfur droplet.

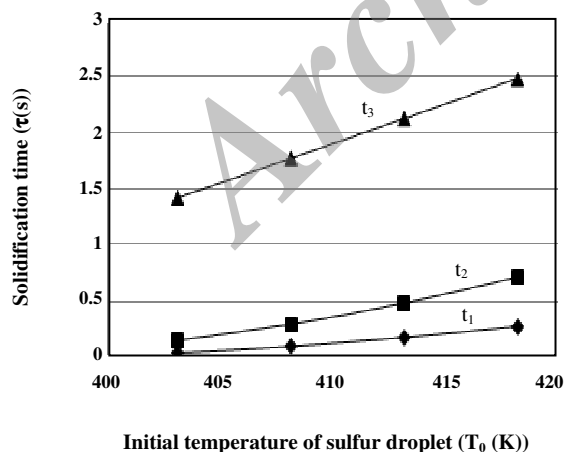


Fig. 10: Effect of initial liquid sulfur temp. increase on the temp. profiles of sulfur pastille.

its two different faces. Furthermore, the solidification process of the sulfur droplet occurs more rapidly when the ambient air temperature or inlet water temperature were reduced. An experimental test rig and data gathering system is under construction to validate the simulation results.

#### Acknowledgements

The assistance of Khangiran sour gas refinery is acknowledged for their financial support of the project.

#### Nomenclature

A	Area of belt, m <sup>2</sup>
C <sub>p</sub>	Heat capacity, J/(kg K)
h	Coefficient of heat transfer, W/(m <sup>2</sup> K)
i	Index of time
k	Coefficient of thermal conductivity, W/(m K)

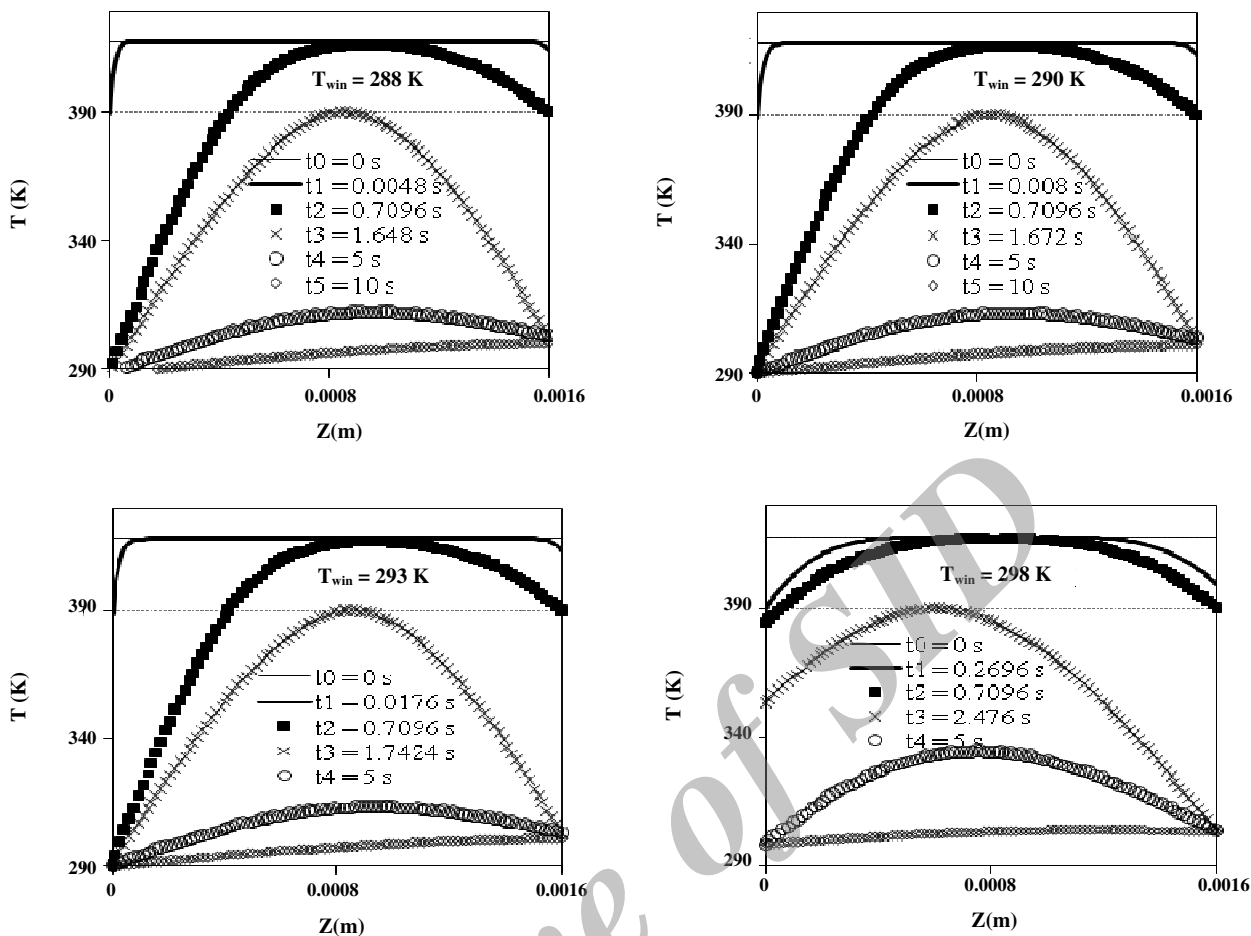


Fig. 11: Various sulfur pastille temp. profiles for different inlet cooling water temperatures.

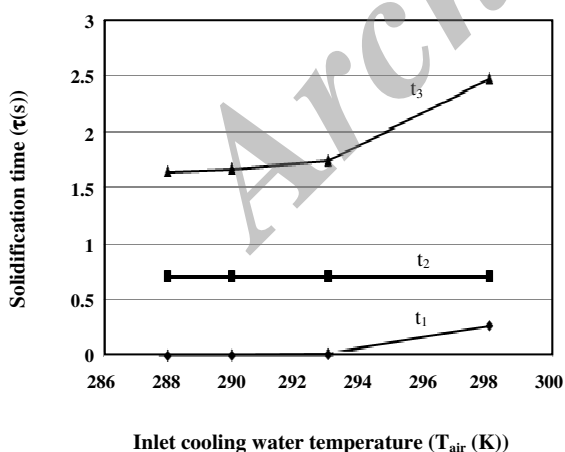


Fig. 12: Effect of inlet cooling water temp. increase on the temp. profiles of sulfur pastille.

l	Liquid phase
lp	Length of pastille, m
ṁ	Mass of water; kg/s
Nu	Nusselt number
Pr	Prandtl number
Q <sub>w</sub>	Heat flux, J/m <sup>2</sup>
Q	Sulfur heat of fusion, J/kg.s
Re	Reynolds number
s	Solid phase
sl	Average of solid and liquid physical properties
T <sub>win</sub>	Inlet cooling water temperature, K
T <sub>wout</sub>	Outlet cooling water temperature K
T <sub>air</sub>	Ambient air temperature, K
T <sub>m</sub>	Solidification (melting) temperature, K
T <sub>0</sub>	Initial liquid sulfur temperature, K
t	Time, S
z	Coordinate of length, m

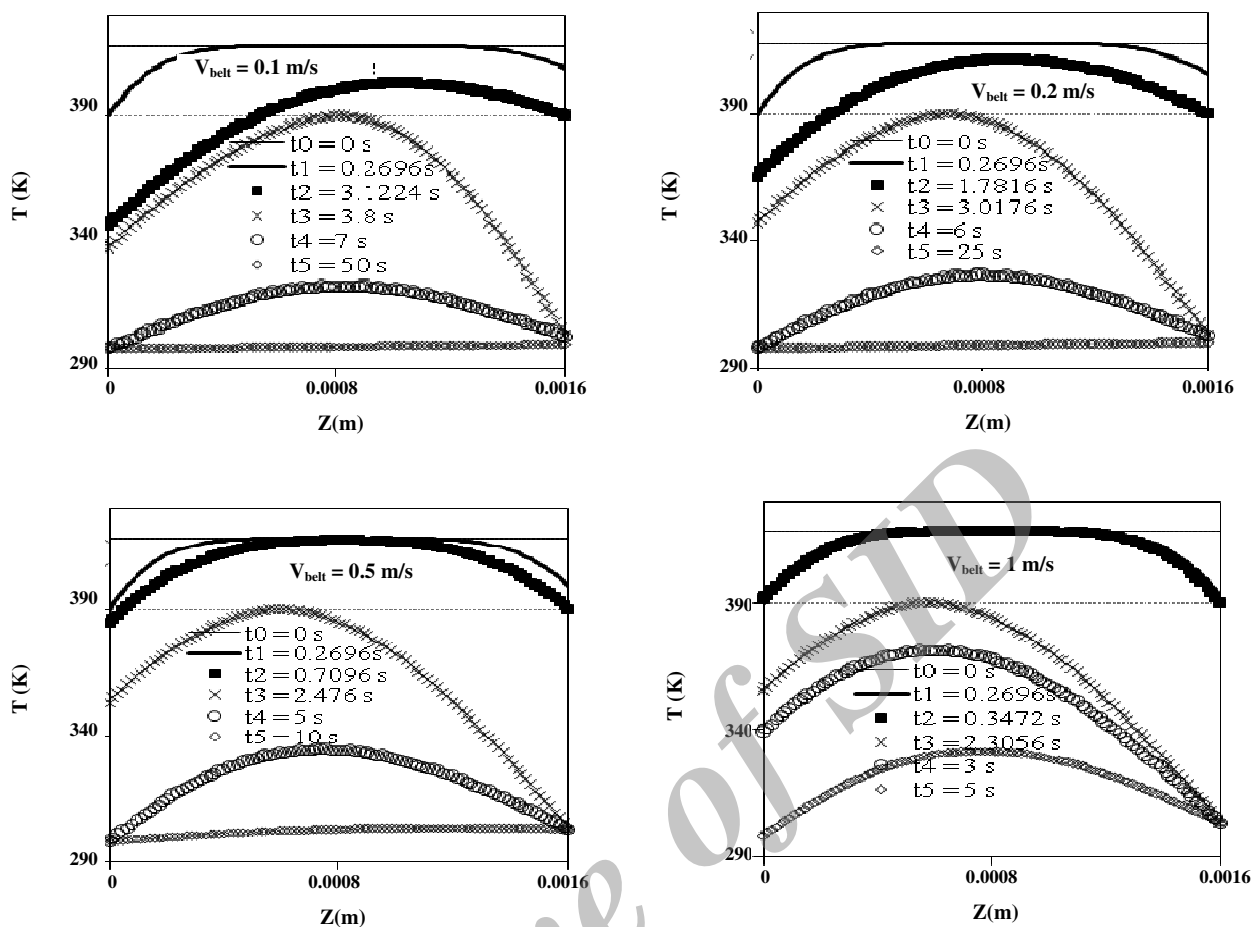


Fig. 13: Various sulfur pastille temperature profiles for different steel belt speeds.

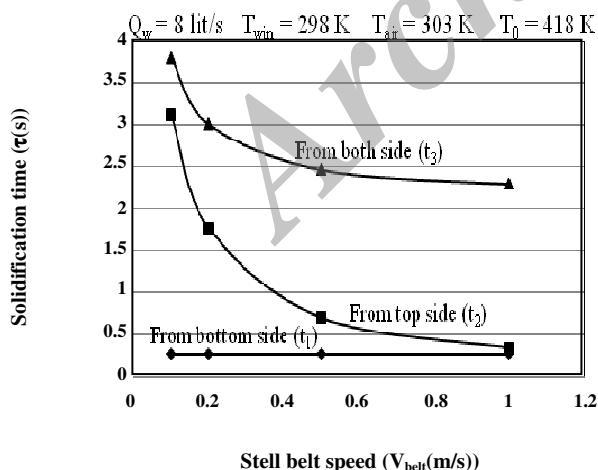


Fig. 14: Effect of steel belt speed increase on the temperature profiles of sulfur pastille.

$\alpha$  Thermal diffusivity,  $m^2/s$   
 $\rho$  Density,  $kg/m^3$

Received : Sep. 27, 2012 ; Accepted : May 6, 2013

REFERENCES

[1] Gang C., "Analysis of Sulfur Granulating Process", Technical Report, Nanjing Sunup Granulation Equipment Company, (2008).  
 [2] Goer B.G., "Sulfur Forming and Degassing Process", Technical Report, Goar, Allison & Associates, Inc, (1983).  
 [3] Gehrman,S., The Pastillation Principle, *J. Hydrocarbon Engineering*, **11**(3), p. 117 (2006).  
 [4] Suh Y., Son G., Numerical Simulation of Droplet Deposition and Self-Alignment on A Microstructured Surface, *J. Numerical Heat Transfer, Part A* , **57**, p. 415 (2010).

- [5] Fang H.S., Bao K., Wei J.A., Zhang H., Wu E.H., Zheng L. L., Simulations of Droplet Spreading and Solidification Using an Improved Sph Model, *J. Numerical Heat Transfer, Part A*, **55**, p. 124 (2009).
- [6] Cantarel A., Lacoste E., Arvieu C., Mantaux O., Danis M., Numerical Simulation of Segregation Phenomena Coupled With Phase Change and Fluid Flow: Application to Metal Matrix Composites Processing, *J. Numerical Heat Transfer, Part A*, **55**, p. 880 (2009).
- [7] Bubnovich V., Quijada E., Reyes A., Computer Simulation Of Atmospheric Freeze Drying of Carrot Slices in A Fluidized Bed, *J. Numerical Heat Transfer, Part A*, **56**, p. 170 (2009)
- [8] Pardeshi R., Singh A.K., Dutta P., Modeling of Solidification Process in A Rotary Electromagnetic Stirrer, *J. Numerical Heat Transfer, Part A*, **55**, p. 42 (2009).
- [9] Mughal M.P., Fawad H., Mufti R., Numerical Thermal Analysis to Study the Effect of Static Contact Angle on the Cooling Rate of a Molten Metal Droplet, *J. Numerical Heat Transfer, Part A*, **49**, p. 95 (2006).
- [10] Jafari A., Seyedein S.H., Haghpanahi M., Modeling of Heat Transfer and Solidification of Droplet/Substrate in Microcasting SDM Process, *J. International Journal of Engineering Science (IUST)*, **19**(5-1), p.187 (2008).
- [11] Fritsching U., Bergmann D., Bauckhage K., Metal Solidification During Spray Forming, *J. International Journal of Fluid Mechanics Research*, **4-6**, p. 623 (1997).
- [12] Sozbir N., Yigit C., Issa R.J., Shi-Chune Y., Guven H. R., Ozcebe S., Multiphase Spray Cooling of Steel Plates Near the Leidenfrost Temperature- Experimental Studies and Numerical Modeling, *J. Atomization and Sprays*, **5**, p. 387 (2010).
- [13] Loulou T., Bardon J.P., Heat Transfer During the Spreading and Solidification of A Molten Metal Droplet on A Cooled Substrate, *J. High Temperature Material Processes (An International Quarterly of High-Technology Plasma Processes)*, **4**(1), p. 69 (2000).
- [14] Vincent S., Caltagirone J. P., Arquis, E., Numerical Simulation of Liquid Metal Particles Impacting onto Solid Substrate: Description of Hydrodynamics Processes and Heat Transfers, *J. High Temperature Material Processes (An International Quarterly of High-Technology Plasma Processes)*, **4**(1), p. 79 (2000).
- [15] Johnson G.J., Sulphur Handling Forming, Storage And Shipping, Proc. 7th Int. Bottom of the Barrel Technology Conference and Exhibition, Athens, *Hydrocarbon World*, **4**(1), p. 55-60 (2009).
- [16] Phinney, R., Wet Granulation Method Generating Sulfur Granules. *US Patent 6331193*, (2001).
- [17] Chalmers W.W., Sulfur Pelletizing, *US Patent 4024210*, (1977).
- [18] Leszczynska H., Gulcz M., Januszewski Z., Godlewski C., Gorczyca Z., Janota N., Method of Granulation of Sulfur, *US Patent 4263012*, (1981).
- [19] Higgins J.T., Sulfur Prilling, *US Patent 4389356*, (1983).
- [20] Hite J.R., Method for Prilling Molten Sulfur, *US Patent 3538200*, (1970).
- [21] Bennett F.W., Process of Prilling Molten Materials, *US Patent 4031174*, (1975).
- [22] Sandvik, Sulfur Technology Review, *J. Hydrocarbon Engineering*, **12**(4), p.74 (2007).
- [23] Lamprecht R., High Performance Granulation. The Versatile and Efficient Rotoform Process, *J. CIT Plus*, **11**(47), p. 47 (2008).
- [24] Selivanov N.V., Yakovlev P.V., Features of Heat Transfer in the Granulation of Sulfur, *J. Journal of Engineering Physics and Thermophysics*, **77**(5), p. 904 (2004).
- [25] Yakovlev P.V., Investigation of Heat Exchange in the Water Granulation of Sulfur, *J. Chemical and Petroleum Engineering*, **41**(3-4), p. 185 (2005).
- [26] Vetterling W.T., Teukolsky S.A., Press W.H., Flannery B.P., "Numerical Recipes (The Art of Scientific Computing)", Cambridge University Press, Cambridge, UK, 2nd ed, Chap 19, (1992).
- [27] Bird R.B., Stewart W.E., Lightfoot E.N., "Transport Phenomena", 2nd ed, Chap 9, John Wiley and Sons, Inc., New York, (2002).
- [28] Treybal R.E., "Mass Transfer Operations", Chap 3, McGraw Hill, Boston, (1980).